Synergy of LPS and Shiga-toxin exposure on the RNA expression program of cultured human umbilical vein endothelial cells

David Svilar[1,2], Martijn A. van der Ent[3], David Siemieniak[2], David Ginsburg[1,2,3,4], Audrey C. Cleuren[2,5]

[1] Department of Pediatrics, University of Michigan, Ann Arbor, MI

[2] Life Sciences Institute, University of Michigan, Ann Arbor, MI

[3]Department of Internal Medicine, University of Michigan, Ann Arbor, MI

[4]Department of Human Genetics, University of Michigan, Ann Arbor, MI

[5] Cardiovascular Biology Research Program, Oklahoma Medical Research Foundation, Oklahoma City, OK

Abstract

Background: Hemolytic uremic syndrome (HUS) is a primary thrombotic microangiopathy that can cause acute renal failure, particularly in children, and is commonly triggered by Shiga toxin-producing *Escherichia coli* (STEC) infection. Although previous *in vitro* studies have shown that Shiga toxin (STX) can directly affect the endothelium, gram-negative bacteria such as *E. coli* also contain lipopolysaccharide (LPS) which is known to independently activate endothelial cells. Furthermore, studies in mice and baboons have shown a synergistic effect of LPS and STX in inducing HUS when administered simultaneously.

Objective: Determine how LPS, STX, or combined LPS/STX treatment affect the gene expression program of endothelial cells.

Methods: Human umbilical vein endothelial cells (HUVECs) were treated with STX, LPS or a combination of STX and LPS for either 4 or 24 hours, after which unbiased RNA sequencing analysis was performed.

Results: Four-hour treatment with LPS resulted in a greater number of differentially expressed genes as compared to treatment with STX. In contrast, 24-hour treatment with LPS or STX induced similar numbers of differentially expressed genes. Dual treatment with both toxins resulted in a synergistic effect, showing significant up- or downregulation of multiple transcripts that were not observed in either single treatment group, particularly at the 24-hour timepoint.

Conclusion: Our data provide a resource for assessing the role of endothelial cell gene expression in the pathogenesis of STEC infection and suggest that the responses of these cells to LPS, STX, or combined LPS/STX treatment are unique and temporally regulated.

Introduction

Hemolytic Uremic Syndrome (HUS) is predominantly caused by infection with Shiga-toxin (STX) producing *Escherichia coli* (STEC) O157:H7. It is the most common primary thrombotic microangiopathy (TMA) worldwide, with the majority of patients developing acute renal failure (1-3). STX-induced damage is thought to activate microvascular endothelial cells (ECs), thereby promoting thrombotic microvascular injury in organs such as the gut, brain, heart, and kidney, with renal histopathology demonstrating glomerular capillary EC thickening, swelling and luminal thrombosis (3). STX can bind circulating white blood cells, which is thought to facilitate the transfer of active STX from the gut to kidney endothelial cells (4). Here, STX binds EC glycosphingolipid globotriaosylceramide (Gb3) and is retrograde transported through the Golgi and endoplasmic reticulum (ER), subsequently disrupting protein synthesis leading to endothelial cell injury (5). Although previous studies have confirmed a key role for Gb3 receptor synthesis in STX entrance and cytotoxicity (6, 7), how STX-induced EC injury promotes HUS is still unknown.

In addition to STX, STEC also produces other toxins, including lipopolysaccharide (LPS), which is known to cause many transcriptional changes independent of STX (8). Interestingly, previous studies have shown that human umbilical vein endothelial cell (HUVEC) survival is decreased during combined LPS and STX treatment (9, 10). *In vivo*, LPS and STX have also been reported to have a greater than additive effect on worsening kidney function, both in mouse and baboon models of HUS (11, 12), with dual LPS/STX treatment of mice resulting in a greater number of significantly altered transcripts in the kidney as compared to individual LPS or STX treatment (11). However, as this latter study evaluated changes in gene expression at the organ level, it is not possible to discern whether those changes occurred within the endothelial compartment specifically. We now report a comprehensive RNA sequencing analysis of the effects of LPS and STX (either alone or in combination) in HUVECs, to mimic the early stages of STEC infection *in vivo*. We show that LPS-induced changes occur more rapidly than those induced by STX, with combined LPS/STX treatment resulting in greater than additive effects on the EC gene expression program as compared to LPS or STX alone.

Methods

Cell culture

Primary pooled HUVECs (Lonza #C2519A) were cultured in supplemented endothelial growth media-2 (Lonza EGM-2 BulletKit, #CC-3162) per the manufacturer's instructions. Holotoxin variant Shiga-toxin 2a (STX2; Phoenix Laboratory at Tufts Medical Center) was dissolved in phosphate buffered saline (PBS, Gibco #10010-023) at a stock concentration of 100 ng/µL and frozen at -80°C in single use vials that were thawed immediately prior to treatment. LPS from *Escherichia coli* 026:B6 was obtained from Sigma (L8274) and dissolved in PBS at a concentration of 500 µg/mL. HUVECs were seeded (passage 2; 50,000 cells/well) in 24-well plates 24 hours prior to treatment with PBS, STX (50 or 5 ng/mL), LPS (2.5 µg/mL), or combined STX and LPS.

RNA isolation and sequencing analysis

After 4 or 24 hours of treatment, cells were washed with ice cold PBS followed by RNA isolation (Takara NucleoSpin RNA) and cDNA conversion using the SMART-Seq v4 Ultra Low Input RNA Kit (Takara, #634892). cDNA amplification, purification, shearing, and quality assessment were completed as previously described (13). Subsequent end repair, adapter ligation and amplification of barcoded cDNA was performed using the KAPA HyperPrep Kit (KK8504) combined with NEXTFLEX-96 DNA Barcodes (NOVA-514105). Quality of sequencing libraries was assessed using an Agilent 2100 Bioanalyzer, and libraries were sequenced as 100 paired-end sequencing reads on the NovaSeq6000. Sequence mapping to the transcriptome (GRCh37 human version 32) and quantification was performed using Salmon (14), with the resulting output being directly loaded into DESeq2 using tximport for downstream normalization and differential expression analysis (15, 16). An average raw read count of 20 per sample was used to filter out low abundant transcripts to reduce background noise prior to differential expression analysis. Of note, transcripts below this filter threshold were predominantly non-protein coding (83.8%), whereas transcripts above the filter threshold were primarily protein coding (87.1%), suggesting the filter was effective at removing background noise while capturing significant changes in gene expression. A false discovery rate (FDR or q-value; (17)) of <0.05 in combination with a $\log_2$ fold change <-1 or >1 was used to define statistically significant differential gene expression. Gene Ontology (GO) analysis was performed on gene lists passing the statistical threshold using the "Search Tool for Retrieval of Interacting Genes/Proteins" (STRING) database (18). Data visualization was performed using R, and Venn diagrams were created online using http://bioinformatics.psb.ugent.be/webtools/Venn/.

Reanalysis of STX treated HUVEC microarray data

Microarray data from a previous study where human dermal neonatal microvascular endothelial cells (HMVECs) were treated with STX ((19): GSE32710) was accessed through the Gene Expression Omnibus

(20) and reanalyzed using the GEO2R webtool, where the same statistical cutoffs used for our RNA sequencing data were used.

Data accessibility

All sequencing data is available through the GEO database (GSE285207).

Results and Discussion

STX- and LPS-induced gene expression changes exhibit significant overlap

RNA-seq data from HUVECs were highly reproducible between biological replicates (Fig 1A), independent of treatment group or timepoint. Approximately 20% of the total genes detected in PBS-treated control HUVECs (2804 out of 14245 genes) showed time-dependent differential gene expression when comparing expression levels at 4-hours versus 24-hour. Although significantly upregulated genes (933 / 2804) did not show enrichment for specific biological processes by GO analysis, significantly downregulated genes (1871 / 2804 genes) showed enrichment for GO terms focused on vascular development and proliferation. This is consistent with the expected senescence observed in primary cells during increased time in culture (21), and the phenotypic drift previously reported for primary ECs grown in culture after being removed from their *in vivo* microenvironment (13). Therefore, all subsequent analyses were performed using vehicle treated controls at the same timepoint as the reference to distinguish toxin-induced changes in gene expression.

Upregulated genes composed the majority of the observed changes following toxin treatment at both time points (Figure 2A-F). Gene expression changes relative to PBS controls were similar for HUVEC treated with either 5 or 50 ng/ml STX at the 4-hour time point (Figure 1B). At 24-hours, a clear distinction between 5 or 50 ng/ml STX could be made, with STX 50ng/mL exhibiting a greater change in gene expression (Figure 1C). Therefore, we focused our analysis on this latter treatment group. Compared to PBS controls, LPS induced rapid changes in mRNA expression, with 1109 differentially expressed genes observed after 4-hour treatment, whereas only 309 genes were differentially expressed after STX treatment at 4 hours (Figure 2G). This is also reflected in the heatmap (Figure 1D), which indicates that the presence of LPS is the main driver of the group clustering. On the other hand, at 24 hours there were 1414 differentially expressed genes in the STX treatment group as compared to 1774

genes in LPS-treated cells, with 583 genes overlapping between the 2 treatment groups (Figure 2H) and STX treatment being the most evident driver of hierarchical clustering analysis (Figure 1E).

GO analysis of the 500 genes with the lowest q-values (17) after LPS treatment was conducted to assess enriched biological processes. As expected, LPS treatment resulted in differentially expressed genes associated with inflammatory processes and EC activation, which was sustained at the 24-hour timepoint. Interestingly, GO analysis of genes significantly affected by STX identified inflammatory processes limited to lymphocyte activation. For example, our data showed significant upregulation of TNF and IL6 with LPS treatment at both 4- and 24-hours, but not with STX treatment alone. As prior studies have shown that TNF and IL6 levels correlate with HUS severity and development of extrarenal complications (22), our results suggest that the LPS-induced inflammatory response in STEC infection likely directly contributes to HUS development.

STX treatment on the other hand, resulted in significantly upregulated transcripts overrepresented in GO terms focusing on the ER stress response and p38/MAPK signaling at 24 hours (Table 1). This is potentially due to STX-mediated protein synthesis inhibition inducing ER stress, consistent with previously reported findings that p38/MAPK signaling is essential for STX-induced increases in macrophage cytokine production (23, 24). ECs are known to increase cytokine production in response to bacterial toxins such as STX and LPS (25), which may also depend on p38/MAPK signaling. To assess whether these STX-induced changes were unique to HUVECs, we compared our data to a previously published study characterizing the response to 24-hour STX treatment in HMVECs, as evaluated by microarray analysis (19). The HMVECs used in the prior study were of dermal origin and composed of only microvascular ECs, thus differing from HUVECs in both the size of the vessel these ECs were isolated from as well as the tissue of origin. Although only 57 genes showed statistically significant differences in the HMVEC study, 35 of these genes overlap with our 24h STX treatment data. GO analysis of these 35 transcripts also identified enrichment for regulation of the p38/MAPK cascade, suggesting that this pathway is part of a general response to STX that is independent of EC origin.

LPS facilitates STX binding to the cell surface by increasing Gb3 receptor expression in specific EC populations, including HUVECs (9). We observed a significant increase in both *UGCG* and *B4GALT5*, the 2 enzymes preceding the final enzyme to synthesize Gb3 (*A4GALT*), with LPS treatment. However, there was no significant difference in *A4GALT* expression between any of the treatment conditions. These data suggest the possibility that the previously reported increase in Gb3 in HUVECs after LPS treatment is due to differential expression of *UGCG* and *B4GALT5*, but not *A4GALT,* which may result in additional

STX sensitivity with dual treatment. In this regard, renal ECs, a presumed primary STX target in HUS, have been reported to express 50x higher Gb3 at baseline and are more sensitive to STX than HUVECs, yet do not exhibit an increase in Gb3 or STX binding following LPS treatment (9). However, dual LPS/STX treatment has been shown to be synergistic in inducing HUS in both mouse (11, 26) and baboon models (12), thus suggesting that LPS treatment is conferring additional kidney EC sensitivity, despite significant Gb3 receptor present at baseline on renal ECs.

Combined STX and LPS treatment have synergistic effects on gene expression

Since STEC produces both LPS and STX, we wanted to further test this potential interaction by treating cells simultaneously with both toxins. This led to significant expression changes in a unique subset of genes at 4 and 24 hours (Figure 2). Given the lower number of gene expression changes induced by STX at 4-hours, combined STX/LPS treatment had similar gene expression changes as compared to LPS treatment alone. This is also indicated by the overlap of data points in 4-hour PCA (Figure 1B), heatmap clustering (Figure 1D) and similar GO term enrichment, with 13 of the top 15 GO terms being identical. In contrast, of the total of 3940 genes differentially expressed at 24 hours following exposure to LPS, STX, or STX/LPS, 1335 were uniquely altered only in the combined treatment (Figure 2H). Pathway analysis of the 2057 genes upregulated after 24-hour dual STX/LPS treatment revealed enrichment of the unfolded protein response, p38/MAPK, NF-κB, and p-ERK signaling, whereas the 1360 transcripts downregulated by LPS/STX were associated with DNA repair and replication (Table 2). This latter finding suggests a decrease in cellular replication, which correlates with a prior report demonstrating that STX-treated cells slow their cell cycle progression (27).

Additional gene expression changes that may impact HUS pathogenesis include the IL10 signaling pathway that was upregulated in our 24-hour STX/LPS treatment and not at 4-hour treatment. A prior study demonstrated that IL10 deficient mice exhibit fewer neutrophils recruited to the kidney and increased survival in a HUS mouse model compared to control mice (28). LPS-induced inflammation may increase white blood cell delivery of STX to the kidney, contributing to renal EC STX-induced damage and HUS (4). Thus, LPS-induced IL10 secretion may contribute to LPS/STX synergistic toxicity by promoting neutrophil migration to the kidney and increased STX delivery to renal EC.

Although the STX-induced expression changes are delayed as compared to LPS effects in our HUVEC data, the synergistic differential gene expression changes may be responsible for the delay in TMA development. With both LPS and STX present during STEC infection, our data characterizing the

synergistic EC expression changes with dual LPS/STX treatment provide a valuable resource for future examination of the pathophysiology of HUS and may represent a more accurate model of STEC induced differential gene expression than exposure to LPS or STX alone.

References

1. Tarr PI, Gordon CA, Chandler WL. Shiga-toxin-producing Escherichia coli and haemolytic uraemic syndrome. Lancet. 2005;365(9464):1073-86.
2. Flynn JT. Causes, management approaches, and outcome of acute renal failure in children. Curr Opin Pediatr. 1998;10(2):184-9.
3. Freedman SB, van de Kar NCAJ, Tarr PI. Shiga Toxin-Producing. N Engl J Med. 2023;389(15):1402-14.
4. Niu S, Paluszynski J, Bian Z, Shi L, Kidder K, Liu Y. LPS-primed CD11b+ leukocytes serve as an effective carrier of Shiga toxin 2 to cause hemolytic uremic syndrome in mice. Sci Rep. 2018;8(1):3994.
5. Tsai HM. The molecular biology of thrombotic microangiopathy. Kidney Int. 2006;70(1):16-23.
6. Pacheco AR, Lazarus JE, Sit B, Schmieder S, Lencer WI, Blondel CJ, et al. CRISPR Screen Reveals that EHEC's T3SS and Shiga Toxin Rely on Shared Host Factors for Infection. MBio. 2018;9(3).
7. Yamaji T, Sekizuka T, Tachida Y, Sakuma C, Morimoto K, Kuroda M, et al. A CRISPR Screen Identifies LAPTM4A and TM9SF Proteins as Glycolipid-Regulating Factors. iScience. 2019;11:409-24.
8. Mullins GE, Sunden-Cullberg J, Johansson AS, Rouhiainen A, Erlandsson-Harris H, Yang H, et al. Activation of human umbilical vein endothelial cells leads to relocation and release of high-mobility group box chromosomal protein 1. Scand J Immunol. 2004;60(6):566-73.
9. Obrig TG, Louise CB, Lingwood CA, Boyd B, Barley-Maloney L, Daniel TO. Endothelial heterogeneity in Shiga toxin receptors and responses. J Biol Chem. 1993;268(21):15484-8.
10. Louise CB, Obrig TG. Shiga toxin-associated hemolytic uremic syndrome: combined cytotoxic effects of shiga toxin and lipopolysaccharide (endotoxin) on human vascular endothelial cells in vitro. Infect Immun. 1992;60(4):1536-43.
11. Keepers TR, Psotka MA, Gross LK, Obrig TG. A murine model of HUS: Shiga toxin with lipopolysaccharide mimics the renal damage and physiologic response of human disease. J Am Soc Nephrol. 2006;17(12):3404-14.
12. Siegler RL, Pysher TJ, Lou R, Tesh VL, Taylor FB. Response to Shiga toxin-1, with and without lipopolysaccharide, in a primate model of hemolytic uremic syndrome. Am J Nephrol. 2001;21(5):420-5.
13. Cleuren ACA, van der Ent MA, Jiang H, Hunker KL, Yee A, Siemieniak DR, et al. The in vivo endothelial cell translatome is highly heterogeneous across vascular beds. Proc Natl Acad Sci U S A. 2019;116(47):23618-24.
14. Patro R, Duggal G, Love MI, Irizarry RA, Kingsford C. Salmon provides fast and bias-aware quantification of transcript expression. Nat Methods. 2017;14(4):417-9.
15. Soneson C, Love MI, Robinson MD. Differential analyses for RNA-seq: transcript-level estimates improve gene-level inferences. F1000Res. 2015;4:1521.
16. Love MI, Huber W, Anders S. Moderated estimation of fold change and dispersion for RNA-seq data with DESeq2. Genome Biol. 2014;15(12):550.
17. Benjamini Y, Hochberg Y. Controlling the False Discovery Rate: A Practical and Powerful Approach to Multiple Testing. Journal of the Royal Statistical Society Series B (Methodological). 1995;57(1):289-300.
18. Szklarczyk D, Kirsch R, Koutrouli M, Nastou K, Mehryary F, Hachilif R, et al. The STRING database in 2023: protein-protein association networks and functional enrichment analyses for any sequenced genome of interest. Nucleic Acids Res. 2023;51(D1):D638-D46.
19. Petruzziello-Pellegrini TN, Yuen DA, Page AV, Patel S, Soltyk AM, Matouk CC, et al. The CXCR4/CXCR7/SDF-1 pathway contributes to the pathogenesis of Shiga toxin-associated hemolytic uremic syndrome in humans and mice. J Clin Invest. 2012;122(2):759-76.
20. Edgar R, Domrachev M, Lash AE. Gene Expression Omnibus: NCBI gene expression and hybridization array data repository. Nucleic Acids Res. 2002;30(1):207-10.

21. Hayflick L, Moorhead PS. The serial cultivation of human diploid cell strains. Experimental Cell Research. 1961;25(3):585-621.
22. Fernández GC, Ramos MV, Landoni VI, Bentancor LV, Fernández-Brando RJ, Exeni R, et al. Cytokine production is altered in monocytes from children with hemolytic uremic syndrome. J Clin Immunol. 2012;32(3):622-31.
23. van Setten PA, Monnens LA, Verstraten RG, van den Heuvel LP, van Hinsbergh VW. Effects of verocytotoxin-1 on nonadherent human monocytes: binding characteristics, protein synthesis, and induction of cytokine release. Blood. 1996;88(1):174-83.
24. Cherla RP, Lee SY, Mees PL, Tesh VL. Shiga toxin 1-induced cytokine production is mediated by MAP kinase pathways and translation initiation factor eIF4E in the macrophage-like THP-1 cell line. J Leukoc Biol. 2006;79(2):397-407.
25. Shao Y, Saredy J, Yang WY, Sun Y, Lu Y, Saaoud F, et al. Vascular Endothelial Cells and Innate Immunity. Arterioscler Thromb Vasc Biol. 2020;40(6):e138-e52.
26. Ikeda M, Ito S, Honda M. Hemolytic uremic syndrome induced by lipopolysaccharide and Shiga-like toxin. Pediatr Nephrol. 2004;19(5):485-9.
27. Suardana IW, Swacita IBN, Pinatih KJP, Suharsono H, Widiasih DA. Assessment of Cell Cycle and Induction of Apoptosis by Shiga-like Toxin Produced by Escherichia coli O157:H7 in T47D Breast Cancer Cells Using Flow Cytometry. Asian Pac J Cancer Prev. 2022;23(10):3247-52.
28. Pineda GE, Rearte B, Todero MF, Bruballa AC, Bernal AM, Fernandez-Brando RJ, et al. Absence of interleukin-10 reduces progression of shiga toxin-induced hemolytic uremic syndrome. Clin Sci (Lond). 2021;135(3):575-88.

Figure Legends

Figure 1: HUVECs treated with STX, LPS or dual treatment exhibit significant overlap of differentially expressed genes. Principal component analysis of vehicle, STX, LPS, and combined STX/LPS treatment at both (A) 4 and 24-hours, (B) 4-hours only, or (C) 24-hours only. Heatmap plotting the $\log_2$ fold change compared to vehicle controls, across treatments (columns) and individual genes (rows) for (D) 4-hours and (E) 24-hour treatment.

Figure 2: Volcano plots with differential expression plotted on the x-axis ($\log_2$ fold change of experimental condition compared to control), and statistical significance on the y-axis ($-\log_{10}$ of the q-value). Dashed lines demarcate the statistical cutoffs ($\log_2$ fold change <-1 or >1, q-value <0.05). Significantly differentially expressed genes (red), and genes not reaching the significance threshold (gray) were plotted for (A) STX 50 ng/mL at 4-hours, (B) STX 50ng/mL and LPS at 4-hours, (C) LPS at 4-hours, (D) STX 50ng/mL at 24-hours, (E) STX 50ng/mL and LPS at 24-hours, and (F) LPS at 24-hours. Venn diagrams display the overlap of differentially expressed genes between the different treatments compared to PBS controls at (G) 4-hours and 24-hours (H).

Figure 1

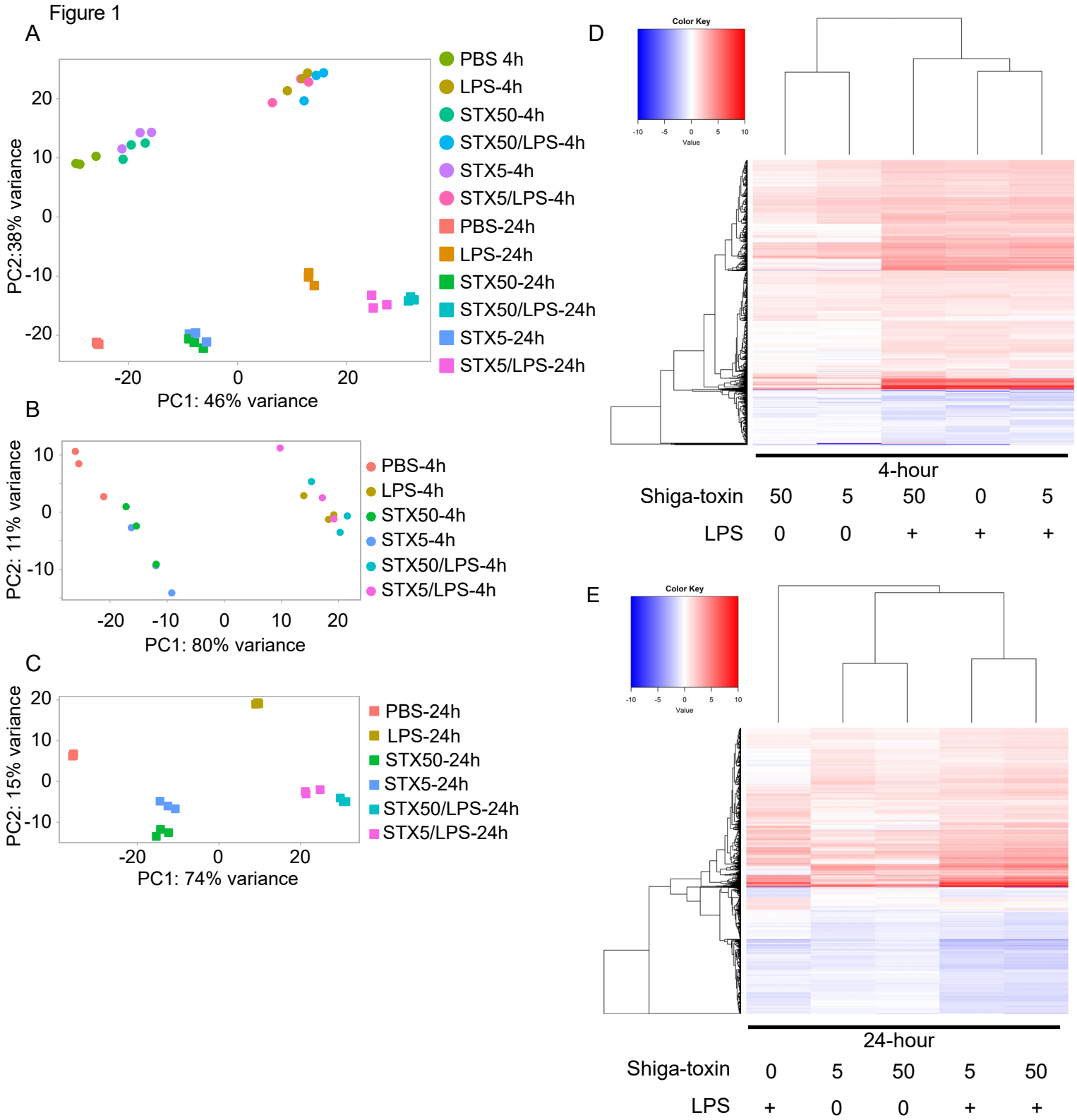
A
PC2:38% variance
PC1: 46% variance
PBS 4h
LPS-4h
STX50-4h
STX50/LPS-4h
STX5-4h
STX5/LPS-4h
PBS-24h
LPS-24h
STX50-24h
STX50/LPS-24h
STX5-24h
STX5/LPS-24h
B
PC2: 11% variance
PC1: 80% variance
PBS-4h
LPS-4h
STX50-4h
STX5-4h
STX50/LPS-4h
STX5/LPS-4h
C
PC2: 15% variance
PC1: 74% variance
PBS-24h
LPS-24h
STX50-24h
STX5-24h
STX50/LPS-24h
STX5/LPS-24h
D
Color Key
Value
4-hour
Shiga-toxin 50 5 50 0 5
LPS 0 0 + + +
E
Color Key
Value
24-hour
Shiga-toxin 0 5 50 5 50
LPS + 0 0 + +

Figure 2

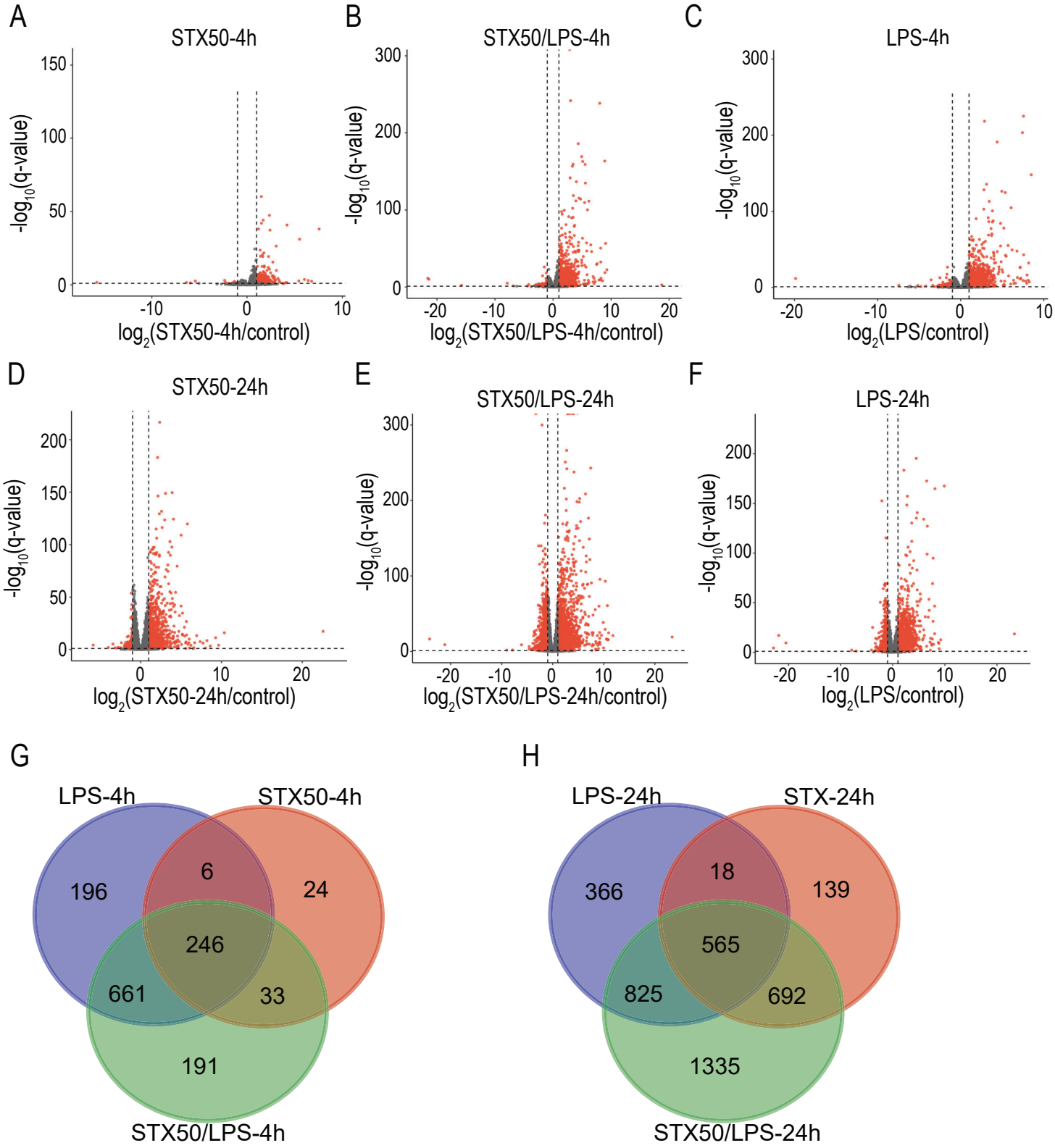
A
STX50-4h
-log10(q-value)
log2(STX50-4h/control)
B
STX50/LPS-4h
-log10(q-value)
log2(STX50/LPS-4h/control)
C
LPS-4h
-log10(q-value)
log2(LPS/control)
D
STX50-24h
-log10(q-value)
log2(STX50-24h/control)
E
STX50/LPS-24h
-log10(q-value)
log2(STX50/LPS-24h/control)
F
LPS-24h
-log10(q-value)
log2(LPS/control)
G
LPS-4h
STX50-4h
STX50/LPS-4h
196
6
24
246
661
33
191
H
LPS-24h
STX-24h
STX50/LPS-24h
366
18
139
565
825
692
1335

Table 1: GO terms associated with significantly differentially expressed genes after 24-hour STX

GO term description	Strength	FDR	Proteins in network
Positive regulation of endoplasmic reticulum stress-induced intrinsic apoptotic signaling pathway	1.21	0.0155	SIRT1, PMAIP1, BBC3, DDIT3
Histone H3 deacetylation	1.14	0.0243	SIRT1, PER1, SFPQ, HDAC9
Inositol phosphate biosynthetic process	1.1	0.0292	ITPKC, IPPK, IPMK, ITPKB
Regulation of CD8-positive, alpha-beta T cell activation	1.07	0.01	IRF1, SH3RF1, RUNX1, CD274, CBFB
Nucleolus organization	1.07	0.035	RRN3, SIRT1, RRP8, USP36
Integrated stress response signaling	1	0.0016	JUNB, FOS, EIF2AK3, FOSL1, ATF4, CEBPD, DDIT3
Positive regulation of miRNA transcription	0.92	0.00046	NR3C1, EGR1, FOS, FOSL1, SMAD3, FOXO3, KLF4, BMP2, ETS1
Adrenal gland development	0.92	0.0324	NR3C1, ARID5B, SMAD3, CITED2, CYP1B1
Positive regulation of transcription by RNA polymerase I	0.91	0.0121	IPPK, BNC1, EIF2AK3, ATF4, DDX21, WDR43
Regulation of p38MAPK cascade	0.89	0.0052	GADD45B, DUSP1, PER1, DUSP10, GADD45A, BMP2, CYLD
Regulation of endoplasmic reticulum stress-induced intrinsic apoptotic signaling pathway	0.89	0.0137	SIRT1, EIF2AK3, PMAIP1, PTPN1, BBC3, DDIT3
Positive regulation of vascular endothelial growth factor production	0.88	0.0407	IL1A, EIF2AK3, ATF4, IL6, CYP1B1
Positive regulation of response to endoplasmic reticulum stress	0.86	0.0194	SIRT1, PMAIP1, PTPN1, ERN1, BBC3, DDIT3
Temperature homeostasis	0.86	0.0496	EGR1, NR1D1, IL1A, ADRB2, SQSTM1
Placenta blood vessel development	0.86	0.0496	MAPK1, HES1, JUNB, FOSL1, HEY2

treatment, ranked by enrichment strength.

Table 2: LPS/STX treatment for 24-hours decreased gene expression in GO terms related to

GO term description	strength	FDR	Proteins in network
Regulation of acyl-CoA biosynthetic process	1.51	0.0107	PDK4, PDK2, PDK3, SNCA
Positive regulation of DNA-directed DNA polymerase activity	1.27	0.0016	GINS2, CHTF18, DSCC1, PCNA, RFC4, RFC5
Response to folic acid	1.26	0.0363	BCHE, MGMT, TYMS, CBS
Double-strand break repair via break-induced replication	1.23	0.0107	MCM5, GINS2, MCM2, CDC7, MCM3
L-serine metabolic process	1.23	0.0107	SHMT1, PSAT1, PSPH, CBS, PHGDH
Serine family amino acid biosynthetic process	1.13	0.0016	SHMT1, CTH, PSAT1, PSPH, CBS, DHFR, PHGDH
Primary alcohol catabolic process	1.1	0.0238	SULT1E1, ALDH2, SULT1C4, AKR1C3, SULT1A1
DNA unwinding involved in DNA replication	1.04	0.0116	MCM5, GINS2, RPA1, MCM2, MCM3, RAD51
Nuclear DNA replication	1.01	0.0158	GMNN, MCM2, FEN1, PCNA, MCM3, RAD51
DNA replication initiation	0.99	0.0062	CDC6, MCM5, MCM2, PRIM1, ORC1, CCNE2, MCM3
Regulation of DNA-templated DNA replication	0.97	1.11e-05	MCM5, GMNN, E2F8, GINS2, CHTF18, MCM2, DSCC1, PCNA, RFC4, CDC7, RFC5, TIMELESS, MCM3
Basement membrane organization	0.91	0.0363	MMP11, NID2, NID1, SPINT2, COL3A1, NTN4
DNA duplex unwinding	0.77	0.00058	MCM5, GINS2, RPA1, BRIP1, CHTF18, MCM2, DSCC1, ERCC6L, RAD54L, RFC4, RFC5, MCM3, RAD51
Cellular aldehyde metabolic process	0.77	0.0123	ALDH2, MGAT4A, ALDH1A1, IDH2, ALDH3A2, AKR1C3, ALDH7A1, IDH1, ALDH3A1
DNA conformation change	0.74	0.00056	MCM5, GINS2, RPA1, BRIP1, CHTF18, MCM2, DSCC1, ERCC6L, RAD54L, RFC4, RFC5, TOP2A, MCM3, RAD51
DNA-templated DNA replication	0.73	3.37e-05	CDC6, MCM5, GMNN, GINS2, RPA1, MCM2, RRM1, FEN1, PRIM1, ORC1, PCNA, RFC4, TONSL, RFC5, CCNE2, TIMELESS, MCM3, RAD51

DNA repair and replication.